



Quantifying Soundscapes in the Ross Sea, Antarctica Using Long-Term Autonomous Hydroacoustic Monitoring Systems

Sukyong Yun^{1*}, Won Sang Lee¹, Robert P. Dziak², Lauren Roche³, Haruyoshi Matsumoto^{2,3}, Tai-Kwan Lau^{2,3}, Angela Sremba^{2,3}, David K. Mellinger^{2,3}, Joseph H. Haxel⁴, Seung-Goo Kang⁵, Jong Kuk Hong⁵ and Yongcheol Park⁵

¹ Division of Glacial Environment Research, Korea Polar Research Institute, Incheon, South Korea, ² Pacific Marine Environmental Laboratory, National Oceanic and Atmospheric Administration, Newport, OR, United States, ³ Cooperative Institute for Marine Ecosystem and Resources Studies, Oregon State University, Newport, OR, United States, ⁴ Pacific Northwest National Laboratory, Sequim, WA, United States, ⁵ Division of Polar Earth-System Sciences, Korea Polar Research Institute, Incheon, South Korea

OPEN ACCESS

Edited by:

Oscar Schofield,
Rutgers, The State University
of New Jersey, United States

Reviewed by:

Christoph Waldmann,
University of Bremen, Germany
Sebastian Menze,
Norwegian Institute of Marine
Research (IMR), Norway

*Correspondence:

Sukyong Yun
yun@kopri.re.kr

Specialty section:

This article was submitted to
Ocean Observation,
a section of the journal
Frontiers in Marine Science

Received: 30 April 2021

Accepted: 29 September 2021

Published: 04 November 2021

Citation:

Yun S, Lee WS, Dziak RP,
Roche L, Matsumoto H, Lau T-K,
Sremba A, Mellinger DK, Haxel JH,
Kang S-G, Hong JK and Park Y
(2021) Quantifying Soundscapes
in the Ross Sea, Antarctica Using
Long-Term Autonomous
Hydroacoustic Monitoring Systems.
Front. Mar. Sci. 8:703411.
doi: 10.3389/fmars.2021.703411

Deployment of long-term, continuously recording passive-acoustic sensors in the ocean can provide insights into sound sources related to ocean dynamics, air–sea interactions, and biologic and human activities, all which contribute to shaping ocean soundscapes. In the polar regions, the changing ocean climate likely contributes to seasonal and long-term variation in cryogenic sounds, adding to the complexity of these soundscapes. The Korea Polar Research Institute and the U.S. National Oceanic and Atmospheric Administration have jointly operated two arrays of autonomous underwater hydrophones in the Southern Ocean, one in the Terra Nova Bay Polynya (TNBP) during December 2015–January 2019 and the other in the Balleny Islands (BI) region during January 2015–March 2016, to monitor changes in ocean soundscapes. In the BI region, we found distinct seasonal variations in the cryogenic signals that were attributed to collisions and thermal/mechanical fracturing of the surface sea ice. This is consistent with sea-ice patterns due to annual freeze–thaw cycles, which are not clearly observed in TNBP, where frequent blowing out of sea ice by katabatic winds and icequakes from nearby ice shelves generate strong noise even in austral winters. Another advantage of passive acoustic recordings is that they provide opportunities to measure biodiversity from classifying spectral characteristics of marine mammals: we identified 1. Leopard seals (*Hydrurga leptonyx*; 200–400 Hz), most abundant in the BI region and TNBP in December; 2. Antarctic blue whales (*Balaenoptera musculus*; distinctive vocalization at 18 and 27 Hz), strong signals in austral winter and fall in the BI region and TNBP; 3. Fin whales (*B. physalus*; fundamental frequency in the 15–28 Hz and overtones at 80 and 90 Hz), maximum presence in the BI region during the austral summer and spring months; 4. Antarctic minke whales (*B. bonaerensis*; 100–200 Hz), strongest signals

from June to August in the BI region; 5. Humpback whales in TNBP; 6. Unidentified whales (long-duration downsweeping from 75 to 62 Hz), detected in TNBP. Long-term soundscape monitoring can help understand the spatiotemporal changes in the Southern Ocean and cryosphere and provide a means of assessing the status and trends of biodiversity in the Ross Sea Region Marine Protected Area.

Keywords: passive acoustic monitoring, Southern Ocean, cryogenic signals, air-sea interaction, biodiversity, Marine Protected Area

INTRODUCTION

The ocean soundscape is a combination of underwater sounds from various sources corresponding to a particular location and time, including from marine animals, tectonic activities, ocean dynamics, air-sea interactions, and human activities. The basic concept of underwater sound sources and their acoustic characteristics have been developed in studies on ocean ambient noise (Knudsen et al., 1948; Wenz, 1962). Knudsen et al. (1948) classified the main sources into water motion, marine life, shipping, and other man-made sources, and investigated the ambient noise characteristics (spectra and pressure levels) from these sources. The term “soundscape” was coined by Schafer (1969), who established the World Soundscape Project (WSP) in the late 1960s–early 1970s. These early soundscape studies mainly focused on the ecological field and various interdisciplinary studies (Matsinos et al., 2016).

Listening to sounds and measuring the ocean soundscapes via passive acoustic monitoring (PAM) in the ocean helps understand the physical and biological ocean environment and their interactions. Long-term PAM has revealed that anthropogenic activity (e.g., shipping and seismic surveys) and geophysical noise from stronger winds and icequakes increase ocean ambient noise in the Northern Pacific Ocean (Andrew et al., 2002, 2011; McDonald et al., 2006; Chapman and Price, 2011; Frisk, 2012), Atlantic and Arctic oceans (Moore et al., 2012), Indian Ocean (Miksis-Olds et al., 2013), and the Southern Ocean (Matsumoto et al., 2014; Haver et al., 2017). Increased ocean ambient noise has a negative influence on marine mammal communication and ecological behaviors (Edds-Walton, 1997; Clark et al., 2009; Castellote et al., 2012).

Despite the difficult approach and risks in the recovery of moorings due to sea ice, thousands of hours of underwater acoustic recordings have been made throughout the Southern Ocean south of 60° S since 2001 (Miller et al., 2021). One of the main objectives of this study is to examine the distribution and behavior of endangered Antarctic blue whales (*Balaenoptera musculus intermedia*) and fin whales (*B. physalus*) (Širović et al., 2004; Van Opzeeland et al., 2013). Another objective is to monitor tectonic activities (Dziak et al., 2010) and glacial ice-ocean boundary processes (Pettit, 2012; Pettit et al., 2012; Glowacki et al., 2015; Dziak et al., 2019; Glowacki and Deane, 2020).

In this paper, we give an overview the Southern Ocean soundscape in two different regions of the Western Ross Sea, Antarctica—the Balleny Islands (BI) region, and Terra Nova Bay Polynya (TNBP)—located ~800 km from each other along the eastern Antarctic coastline. We (1) present various biotic

and abiotic sound sources in the BI and TNBP regions in the Ross Sea Marine Protected Area (MPA), (2) show influences of geophysical components (wind speed and sea ice concentration) on the ocean ambient noise and marine mammal vocal activity, and (3) discuss how the geographical differences change the soundscapes in these regions.

DATA AND METHODS

Autonomous Underwater Acoustic Recording System and Mooring

The Korea Polar Research Institute and the U.S. National Oceanic and Atmospheric Administration have jointly monitored the soundscape of the Southern Ocean, specifically in the BI region (January 2015–March 2016) (Figure 1A) and the TNBP (December 2015–January 2019) (Figure 1B) in the Ross Sea.

The BI is a volcanic island chain trending northwest-southeast, and an array of five hydrophones was deployed parallel and to the east of the islands by icebreaker R/V *Araon* in January 2015 and recovered in March 2016. Dziak et al. (2017) found various sound sources (volcano-seismic, cryogenic, and biogenic) in the long-term spectrogram of a hydrophone deployed 400 km north off the coast of the Antarctic continent and 150 km away from the BI. In this study, we analyze the same hydrophone recordings under the identifier BAL15.

In the TNBP, the south and north arrays have been operated along the northeastern edge of the Drygalski Ice Tongue and northern sea-ice margin of the polynya, respectively. The TNB south array was first deployed in December 2015 (Dziak et al., 2019), and there were two recovery/redeployments in February 2017 and March 2018. Final recovery was done in January 2019 by icebreaker R/V *Araon*. The TNB north array was first deployed in February 2017, recovery redeployments were implemented in March 2018, and the recovery was done in January 2019. The locations were changed in every deployment due to the sea ice distribution. Table 1 presents the locations and recording time periods.

The PAM system we used is called Autonomous Underwater Hydrophone (AUH) (Fox et al., 2001). The AUH package deployed in the BI region and TNBP composed of a single ceramic hydrophone, with a filter/amplifier, clock, and a low-power processor called CF2 from Persistor Instrument, which were all powered by an internal battery pack. The hydrophone model was ITC-1032, which is omnidirectional with a nominal sensitivity of -192 dB re 1 V μ Pa $^{-1}$. The instrument continuously

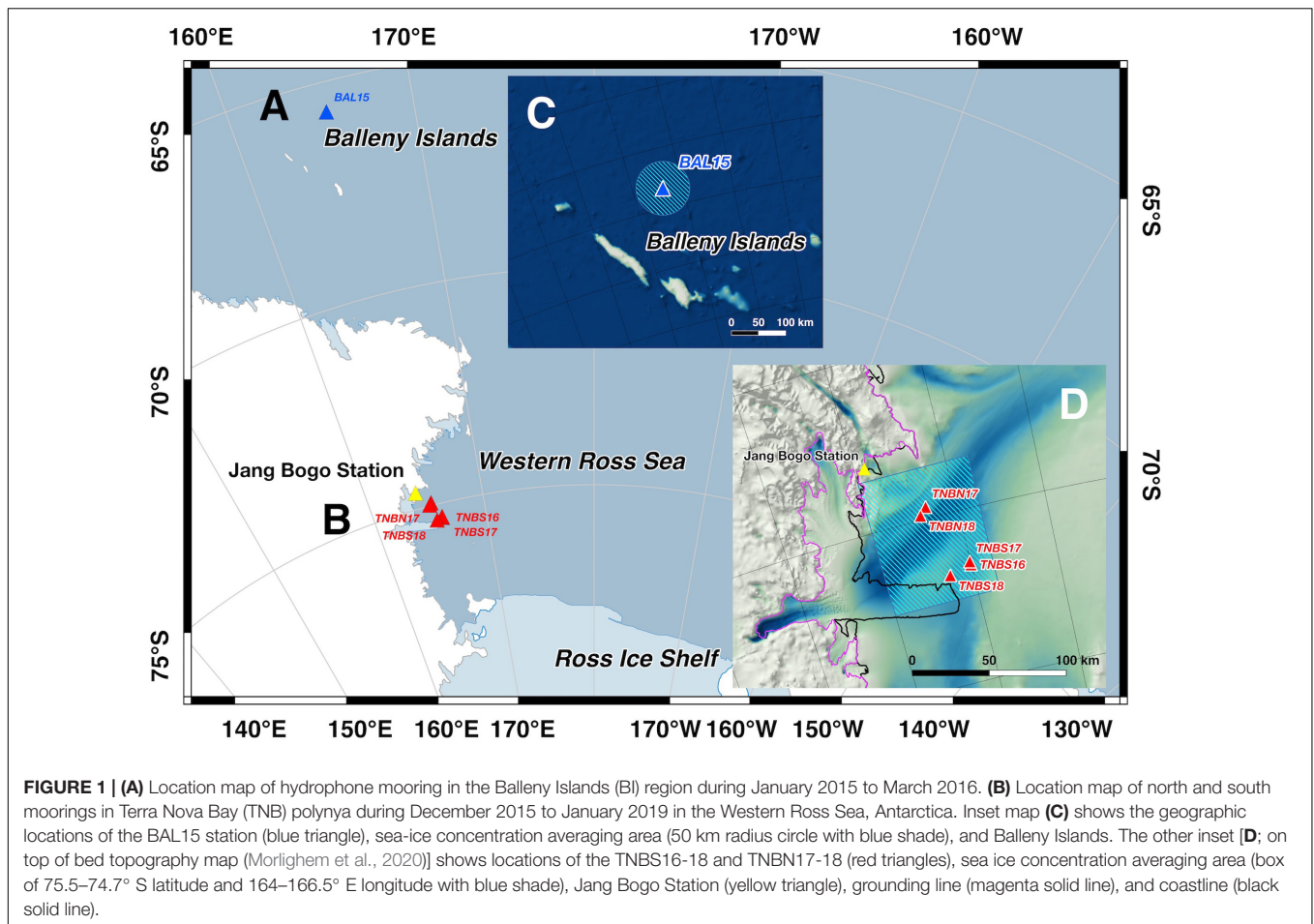
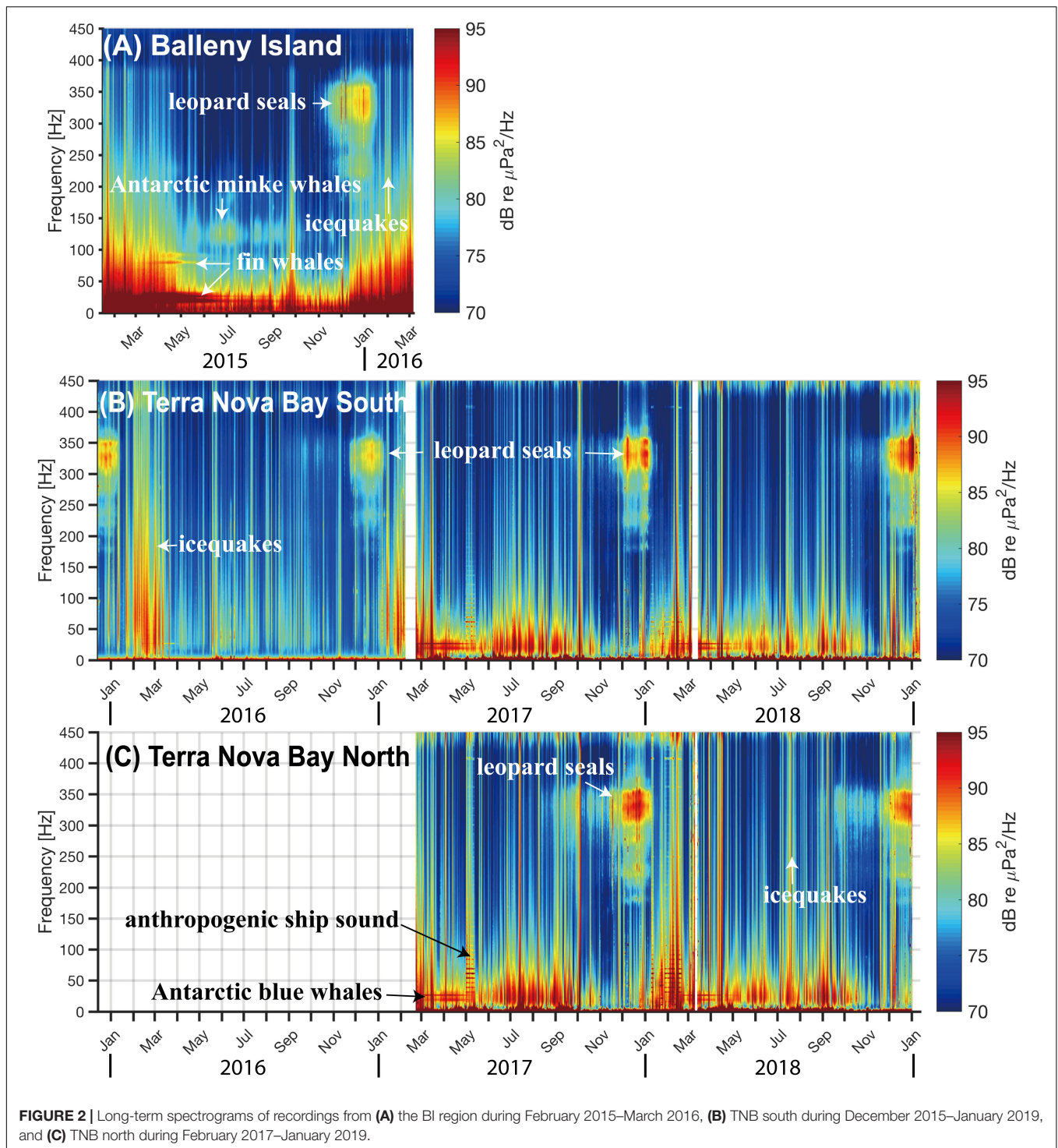


TABLE 1 | Properties of the hydroacoustic records in the BI region and TNB.

Station(Hydrophone ID)	Operation period	Latitude	Longitude
Balleny Islands			
BAL15 (HC02)	2015.01.15~2016.03.07	65° 40.3125' S	165° 12.2823' E
TNB South			
TNBS16 (HC14)	2015.12.12~2017.02.09	75° 19.4016' S	165° 59.4877' E
TNBS17 (HC21)	2017.02.14~2018.03.05	75° 18.2774' S	165° 58.9592' E
TNBS18 (HC25)	2018.03.12~2019.01.13	75° 21.3110' S	165° 28.1400' E
TNB North			
TNBN17 (HC25)	2017.02.05~2018.03.11	74° 55.9911' S	165° 18.8791' E
TNBN18 (HC21)	2018.03.14~2019.01.01	74° 58.5180' S	165° 9.3563' E

records at a sampling rate of 1 kHz with 16-bit resolution. The pre-amplifier has an eight-pole anti-aliasing filter at 400 Hz and has a filter curve to equalize the spectrum against typical ocean noise over the pass-band (Dziak et al., 2019). In the BI region, a microprocessor controlled, temperature-correcting crystal oscillator with an average time drift of 1.95 s year^{-1} was deployed for 1 year (Dziak et al., 2017), and a low-power cesium atomic clock (low power) with an average time drift of $\sim 0.1 \text{ s year}^{-1}$ was used in the TNB array. The electronics were housed in both titanium (for the BI) and fiberglass composite pressure cases (for TNB), and attached to a standard oceanographic mooring

with an anchor, acoustic release, mooring line, and syntactic foam float. The moorings were designed to place the sensor at a depth of 400 m to minimize the chance of iceberg collision. To address the detection ranges of the recorders in the Southern Ocean, we estimate transmission loss of 25 and 400 Hz waves using KRAKEN (Porter, 1992) propagation model for a source at 50 m depth, a receiver at 400 m depth, and sound profiles in the TNBP (**Supplementary Figure 1**). It presents that some of the detected low-frequency signals (e.g., Antarctic blue and fin whale calls with source level of $\sim 189 \text{ dB}$ over 25–29 Hz and 15–28 Hz, respectively; Širović et al., 2007) could originate from 100s of km



away from the recorders, whereas sounds around 400 Hz could have relatively local origins.

Spectral Analysis

All data processing and measurements were performed using MATLAB, 2020b. We calculated the hourly/daily averaged spectrum to (1) characterize the seasonal and regional

variations in the long-term spectrograms (**Figure 2**), (2) quantify the marine mammal contribution to the spectra, and (3) present their diel patterns. Fast Fourier transforms (FFTs) were performed with 1 Hz resolution for a 0% overlapped “Hanning” window of length 1 s (1,000 samples), and the hourly/daily averaged spectral amplitudes were calculated for the entire deployment period. Sources of repeated signals

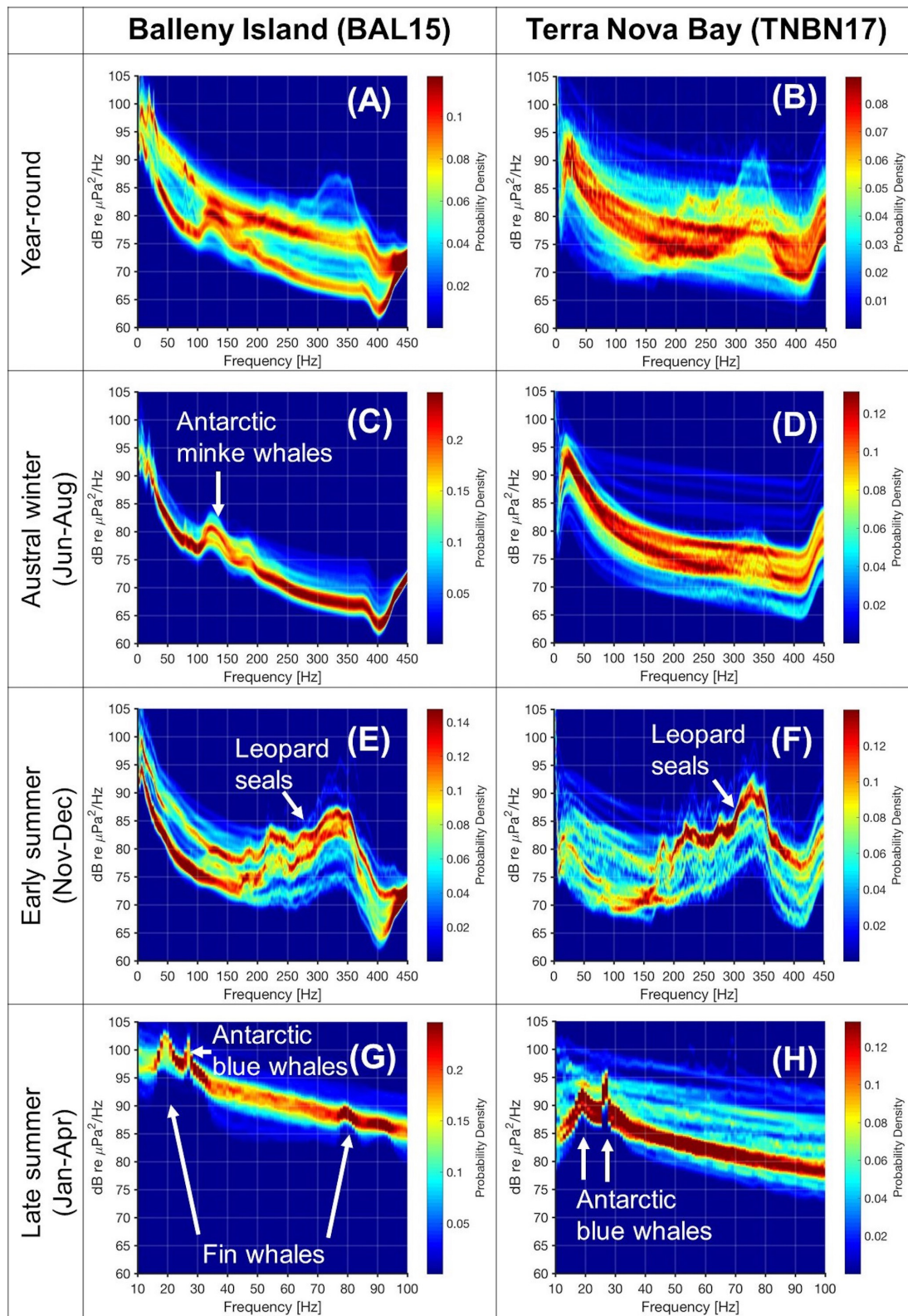


FIGURE 3 | Spectral probability density plots for 1-year records of (A) BAL15 and (B) TNBN17; for austral winter season of (C) BAL15 and (D) TNBN17; for early summer season of (E) BAL15 and (F) TNBN17; and for late summer season of (G) BAL15 and (H) TNBN17.

in the long-term spectrogram are identified by comparing with the characteristics of various sounds in the Southern Ocean reported in previous studies (e.g., Širović et al., 2004; Dziak et al., 2015; Erbe et al., 2017; Menze et al., 2017). Short-duration spectrograms were obtained to verify the exact sound sources by performing FFTs with 1 Hz resolution for a 50% overlap “Hanning” window of 1 s without time averaging (**Supplementary Figure 2**). To identify inter-annual and seasonal characteristics, kernel-smoothed (bin width 0.5) spectral probability densities (SPDs) were estimated from the daily spectra at equally spaced sound levels between 50 and 120 dB (**Figure 3**). Marine mammal contributions (MMC) in the power spectral density (PSD_{MMC}) are calculated for the hourly averaged sound spectra using the method adopted by Menze et al. (2017). We subtract the estimated spectrum without MMC from the measured spectrum. The spectrum without MMC is interpolated by curve fitting with a power function $PSD_{dB} = af^b + c$ (where f is the frequency and a , b , and c are constants determined by fitting). The core frequency bands for the subtracted and fitted frequency bands are chosen from the BI and TNB data that reflect their own frequency response and ambient noise characteristics (**Table 2** and **Supplementary Figure 3**). The PSD_{MMC} value is estimated only when the signal to the background noise ratio of MMC is higher than 1 dB (Menze et al., 2017).

Sea Ice Concentration and Wind Speed Data

Sea-ice concentration data were obtained from the Arctic Radiation and Turbulence Interaction Study with a grid spacing of 3.125 km resolved from the Advanced Microwave Scanning Radiometer 2 (AMSR-2) dataset (Spreen et al., 2008). For the BI region, we averaged the values within a 50 km radius of the BAL15 mooring location (shaded circle in **Figure 1C**). This criterion was used in a previous soundscape study of the Southern Ocean (Menze et al., 2017). For TNBP, the daily averaged sea-ice concentration was calculated in a rectangular area with coordinates 75.5–74.7° S latitude and 164–166.5° E longitude (shaded area in **Figure 1D**). TNBP is a coastal latent heat polynya in the western sector of the Ross Sea, Antarctica. The Drygalski Ice Tongue, located at the southern boundary of the polynya, blocks sea ice moving in from the south, and strong katabatic winds from the Nansen Ice Shelf (NIS) frequently push sea ice away from the coast and create open waters even in the winter season (Kurtz and Bromwich, 1985; Fusco et al., 2002; Sansiviero et al., 2017; Stevens et al., 2017). Considering the high mobility of sea ice in the polynya, we set the masking area to cover all hydrophones and surrounding oceans in the polynya. In addition to sea ice concentration, the monthly sea-ice extent was obtained from the National Snow and Ice Data Center (Fetterer et al., 2002) and was used to estimate the distance between the BAL15 station and the nearest open sea.

The daily wind speed in TNB was calculated from meteorological observations obtained using the Automatic Synoptic Observation System (ASOS) at Jang Bogo Station

(74° 37.4' S, 164° 13.7' E) from December 2015 to December 2018. The daily wind speed in the BI region was extracted from the European Center for Medium Range Weather Forecasts (ECMWF) climate reanalysis dataset ERA5 (Hersbach et al., 2020).

RESULTS AND DISCUSSION

Ambient Sound Characteristics in the Balleny Islands Region and Terra Nova Bay Polynya

Figures 2A–C show the long-term spectrograms of the recordings from the BI region during February 2015–March 2016, TNB south during December 2015–January 2019, and TNB north during February 2017–January 2019, respectively. We can identify the dominant sound sources composing the soundscapes in a region by finding repeated signals in the spectrogram. The broadband (10–400 Hz) vertical lines in all the three spectrograms are icequakes, cryogenic signals originating from the impact and breakup of surface sea ice, ice shelf, and icebergs (MacAyeal et al., 2008; Dziak et al., 2010, 2015, 2019). The horizontal peaks in the 15–30 Hz band generally associated with fin and/or Antarctic blue whale calls (Watkins et al., 1987; Ljungblad et al., 1998) are shown in both regions. However, the horizontal lines in the 80–90 Hz band, usually from fin whale calls (Širović et al., 2004), are clearly shown only in the BI region, not in the TNB records. The vocalizations of leopard seals (Rogers et al., 1996) are apparent in continuous 200–400 Hz broadband and strongest in 300–370 Hz from October to December in the BI region and TNBP. Strong anthropogenic sounds continued for several days in May of 2017.

Supplementary Figure 2 shows short-term spectrograms detailing various sources in the BI region and TNBP. **Supplementary Figure 2A** shows typical earthquake and icequake signals recorded in the BI region. Acoustic waves generated from earthquakes are referred to as *T*-waves, characterized by low-frequency (<100 Hz) wave trains that continue for tens to hundreds of seconds. Icequakes are impulsive, last for a short duration, and have a broadband frequency content. **Supplementary Figure 2B** is a spectrogram in 1–100 Hz band to scrutinize whale vocalization in the BI region. Lots of short-duration, narrow-band signals exist at 80 Hz, but the frequency is lower than typical upper part of fin whale calls in other part of the Southern Ocean: 89 Hz in the West Antarctic Peninsula in 2002 (Širović et al., 2004), 98 Hz in the Atlantic sector in 2009–2010 (Menze et al., 2017), and 99 Hz in the East Antarctica in 2003 (Širović et al., 2009). Lower part of fin whale calls, usually shown in 15–28 Hz band, are difficult to distinguish individually, owed to the number of signals superposed possibly from fin and/or Antarctic blue whales in the 15–30 Hz band (**Supplementary Figure 2B**; see **Supplementary Figure 4** with different color scale). **Supplementary Figure 2C** shows “bioduck” sounds from Antarctic minke whale (Risch et al., 2014) in the BI region in the frequency band of 100–250 Hz. In **Supplementary Figure 2D**, leopard seal vocalizations with

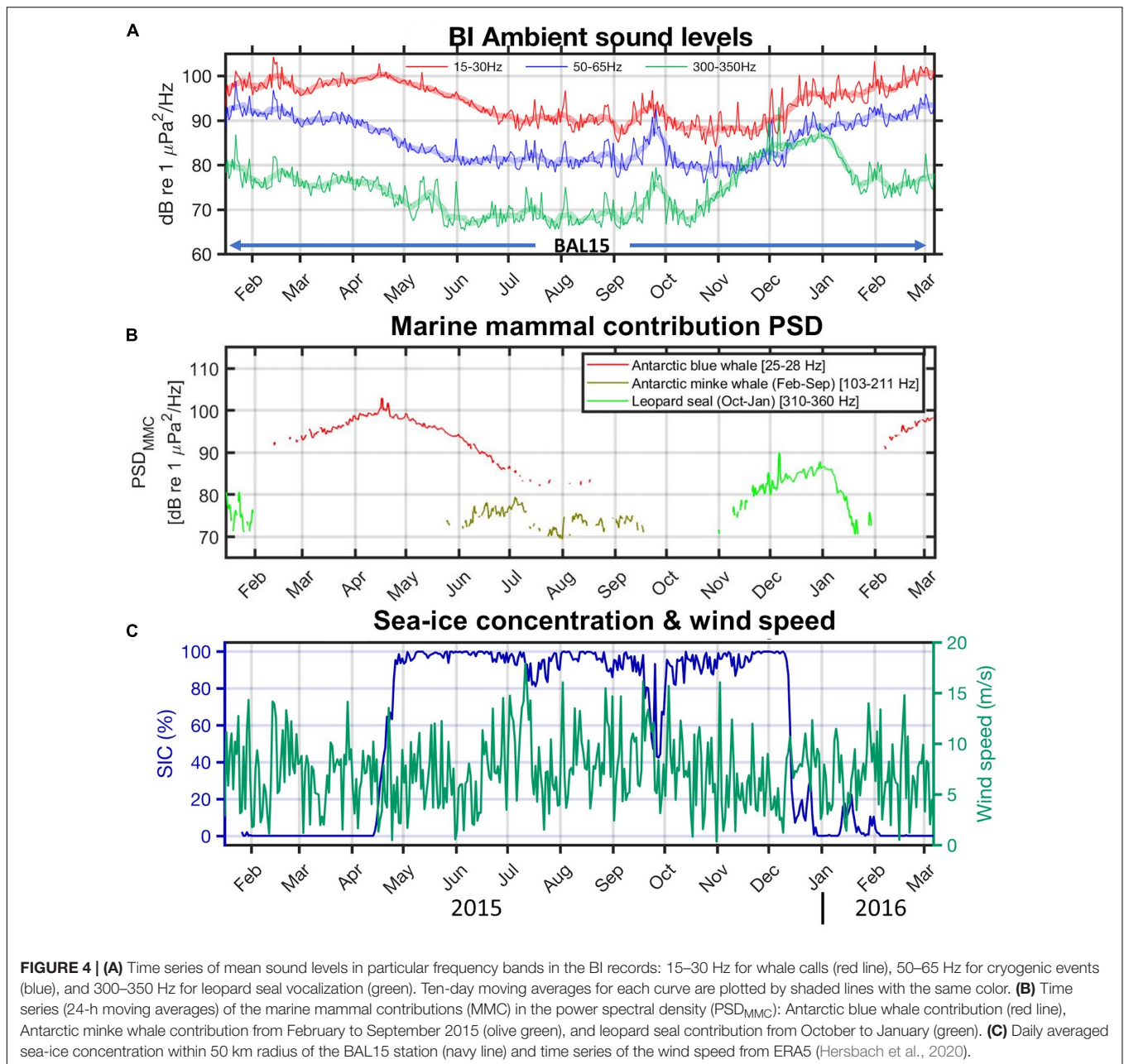


TABLE 2 | Spectral ranges used to calculate PSD_{MMC} . We generally follow the methods adopted by Menze et al. (2017).

	Fitting frequency band	Core frequency range used to calculate PSD_{MMC}	Period limitation	Fitting correlation
Antarctic blue whale in the BI	7–13 and 39–60 Hz	25–28 Hz	–	0.99
Antarctic blue whale in TNB	18–24 and 29–42 Hz	25–28 Hz	–	0.70
Antarctic minke whale in the BI	39–66 and 300–351 Hz	103–211 Hz	Feb–Sep	0.99
Leopard seal in the BI	39–161 and 412–441 Hz	310–360 Hz	Oct–Jan	0.96
Leopard seal in TNB	90–146 and 400–421 Hz	310–360 Hz	–	0.74

Nevertheless, the ranges of core frequency and fitting frequency bands are differently adapted by reflecting the distorted frequency response of the data (Supplementary Figure 3).

TABLE 3 | Slope, intercept, and correlation coefficients for linear fits between sound levels in 50–65 Hz and wind speed for sea-ice concentration data greater than 80% and less than 80%.

	Slope	Intercept (dB)	Pearson's correlation coefficients
BI (SIC > 80%)	0.19	80.0	0.28
BI (SIC < 80%)	0.16	88.9	0.24
TNB (SIC > 80%)	0.61	79.0	0.36
TNB (SIC < 80%)	0.60	79.7	0.37

main energy in the 280–370 Hz band, the “bioduck” sounds from Antarctic minke whale in the 120–250 Hz band, and Antarctic blue whale “D-calls” (Erbe et al., 2017) in the 60–100 Hz band are recorded in TNB in December 2018. **Supplementary Figure 2E** shows a “chorus” of Antarctic blue whales (Thomisch et al., 2016) at around 27 Hz and 18 Hz in the TNB records. **Supplementary Figure 2F** shows that anthropogenic ship noise continued for several days (April 29–13 May, 2017) and noisy status of the ocean continued for several hours during storms in TNB. Strong winds can enhance noise levels through various physical processes, such as higher ocean waves, fracturing and collision of ice blocks, and vibration and fracturing of icebergs and ice shelves (Chaput et al., 2018; Dziak et al., 2019). Humpback whale song in 20–100 Hz band (Payne and McVay, 1971; **Supplementary Figure 2G**) and long-duration (200 s) downsweeps from 75 to 62 Hz (**Supplementary Figure 2H**) were found in TNB in December 2016.

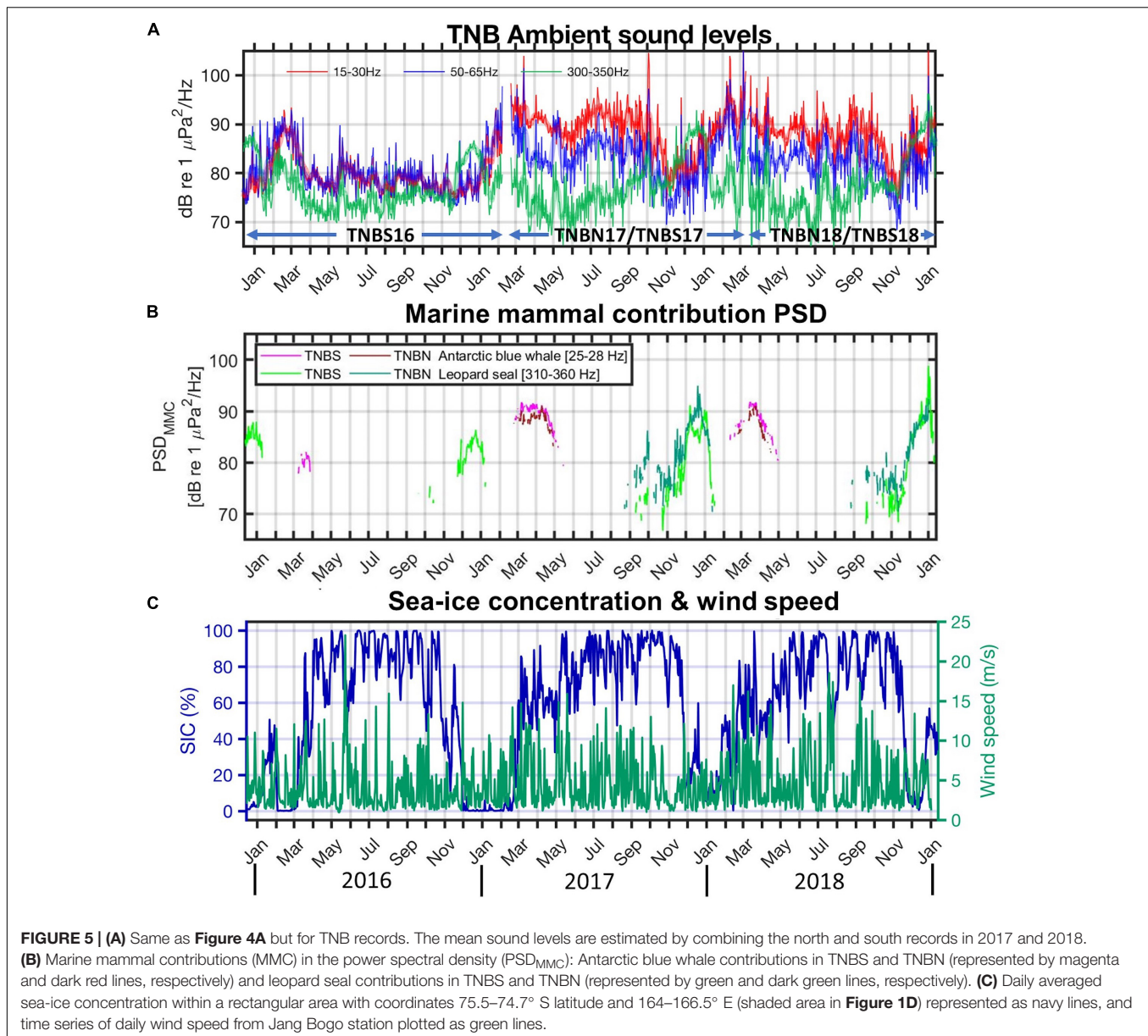
Figure 3 shows the SPDs for the daily averaged spectrum of 1-year deployment records from BAL15 and TNBN17. To determine the seasonal variation in the dominant sound sources for each region, we plotted the SPDs for the entire period (first row; **Figures 3A,B**), austral winter months, June–August (second row; **Figures 3C,D**), early summer months, November–December (third row; **Figures 3E,F**), and late summer, January to April (fourth row; **Figures 3G,H**). The year-round plot in the BI region (**Figure 3A**) shows a bimodal pattern with two separated red lines, and the lower lineation is largely the same as the SPD pattern in the austral winter season in the BI region (**Figure 3C**). This implies that the bimodal pattern in the BI region is a seasonal difference. However, the bimodal pattern in the year-round SPD plot for TNB (**Figure 3B**) is not as clear as that for the BI region, and one of the modes is not shown in any particular seasonal plot. In the SPD of the BI for the austral winter season (**Figure 3C**), sound levels in the 100–200 Hz band increased due to Antarctic minke whale calls. Antarctic minke whales can breathe in dense sea-ice environments by navigating between ice floes and breaking the ice to make breathing holes, and the BI region in austral winter season would be a safe refuge from killer whales (*Orcinus orca*) (Filun et al., 2020). In contrast to the BI region, there was no significant increase in the Antarctic minke whale bands, but leopard seal vocalizations contributed to the frequency band of 280–360 Hz in TNBP even in winter season. The leopard seal calls in the BI region and TNBP were strongest in the early summer season (**Figures 3E,F**). We plotted the SPDs in the late summer season in the frequency band of 10–100 Hz to identify fin and Antarctic blue whale vocalizations.

In the BI region (**Figure 3G**), there are strong peaks at 18 Hz, 27 Hz, and gentle peaks at 80 and 90 Hz. In the BI records, we could not present a spectrogram with clear fin or Antarctic blue whale calls due to the noise in the bands (**Supplementary Figures 2B, 4**). However, the strong peaks at 18 and 27 Hz can be attributed by Antarctic blue whales, as reported in the previous acoustic monitoring in the Ross sea in 2004 (Širović et al., 2009). Meanwhile, the two peaks at 80 and 90 Hz, which are the same frequency bands of the signals shown in **Supplementary Figure 2B**, reveal the existence of fin whales in the region. In the TNB late summer SPD (**Figure 3H**), the amplitude rise is not significant in the overtone fin whale call band (~90 Hz), and the peaks at 18 Hz, 27 Hz associated with the Antarctic blue whale chorus (**Supplementary Figure 2E**) are visible. Another research has identified humpback whale signals off the Antarctic coast at about 70° S (Van Opzeeland et al., 2013), and it is possible that some of the acoustic energy seen in the SPDs of the BI in the 50–300 Hz range is sourced from humpbacks. However, we did not see a definitively identifiable signal in the SPDs for humpback whales; this may be because humpback whale acoustic energy is spread over the spectrum from a few tens of hertz up to several kilohertz rather than being concentrated in a narrow band.

Spectral Amplitude and Its Correlation With Sea Ice and Wind Speed

To address the seasonal variations in the three dominant sound sources (fin and blue whale calls, cryogenic signals, and leopard seal calls) in the BI region and TNBP, mean sound levels were calculated within specific frequency bands: (1) 15–30 Hz for fin and blue whales, (2) 50–65 Hz for cryogenic signals, and (3) 300–350 Hz for leopard seals. Although we selected the 50–65 Hz band for the cryogenic signals where MMC were insignificant in the SPDs (**Figure 3**), the broadband energy from cryogenic signals can strongly affect other marine mammal bands. To address this issue, we estimate spectral levels by calculating MMC to the hourly averaged sound spectra (PSD_{MMC}, Menze et al., 2017). Despite the fact that a lower Nyquist frequency (500 Hz) and intrinsic background fluctuations in the higher frequency range (BI: > 370 Hz, TNB: > 400 Hz) cause disturbances when estimating confident background noise levels in the core frequency band of leopard seals (310–360 Hz, **Table 2**), we practically select upper fitting bands to compare relative time variations in the PSD_{MMC} for each mooring (**Table 2** and **Supplementary Figures 3B,D**).

Figure 4 shows (A) the mean amplitudes of the BI recordings in the specific bands, (B) estimated PSD_{MMC} value, and (C) the geophysical components, sea ice concentration, and wind speed. The mean amplitudes in the 15–30 Hz range (baleen whale band; red line in **Figure 4A**) and PSD_{MMC} value associated with Antarctic blue whales (red line in **Figure 4B**) increase from February to April and turn downward from mid-April; these changes coincide with the rapid increase in sea-ice concentration (navy solid line in **Figure 4C**). The highest levels in April may be related to high densities of krill and greater abundance of baleen whales at the ice margins reported in previous studies



(de la Mare, 1997; Brierley et al., 2002). The PSD_{MMC} value of Antarctic blue whales almost disappeared in July 2015; then they reappeared in February 2016 along with the blue whales' acoustic presence in other Antarctic regions (Širović et al., 2009). The sea ice concentration in the BI region generally remains over 80% from May to November, and the sound levels in most frequency bands decreased during the sea-ice full period. There is an extraordinary event in which the sea ice concentration drops to 50% after a strong storm in late September (Figure 4C), and the sound levels increased in all the frequency bands (Figure 4A). This implies that sea ice coverage is the major factor determining background noise levels in the BI region. The PSD_{MMC} value of Antarctic minke whales (olive green line in Figure 4B) is generally significant from late May to mid-September during the sea-ice full period; however, the PSD_{MMC} value of leopard seals is

the highest from early November to January, which correspond to the breeding season of leopard seals (Southwell et al., 2003).

Figure 5 shows plots similar to those in Figure 4, but for the TNBP during 2016–2018. The mean sound levels were estimated by combining the northern and southern records in 2017 and 2018. Although the narrow amplitude gaps between the bands in 2016 compared with the later period (2017–2018, Figure 5A) implies a poor frequency response correction, we can compare the relative amplitude variation within every deployed period. In 2016, noisy summer (January–March) and silent fall-austral winter-early spring season (April–October) were conspicuous features. Dziak et al. (2019) investigated hundreds of icequakes from the NIS and Campbell glaciers prior to the NIS calving event (April 7, 2016) from January to March 2016. The broadband energy from the icequakes peaked in all the frequency bands

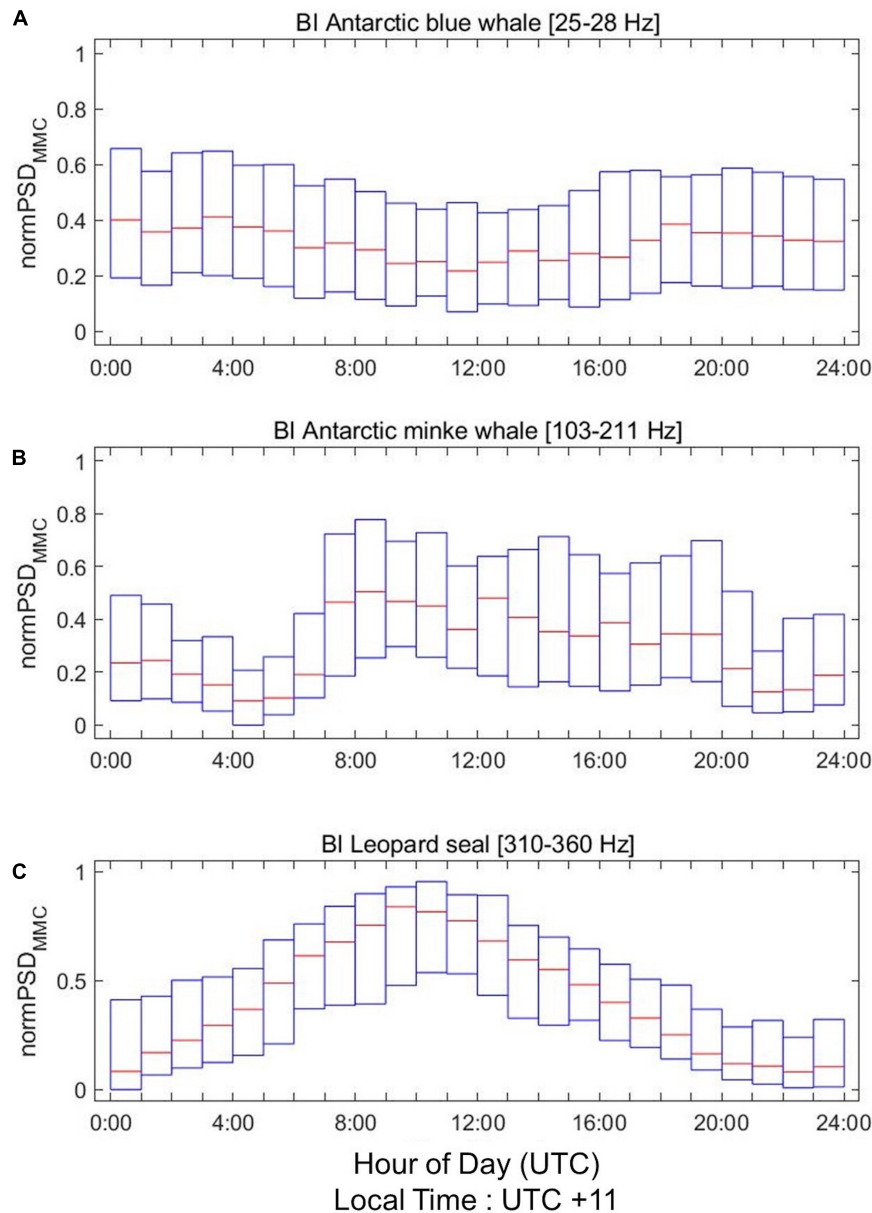


FIGURE 6 | Diel patterns in normalized PSD_{MMC} values of **(A)** Antarctic blue whales, **(B)** Antarctic minke whales (middle), and **(C)** leopard seals (bottom) in the BI region. X axis represents the UTC time, and the local time in the BI region is UTC + 11. Estimated hourly PSD_{MMC} values are normalized between 0 and 1 for each day. Red line indicates the median value, and the bottom and top edges of the box indicate the 25th and 75th percentiles, respectively.

in February 2016 (**Figure 5A**). The seasonal pattern in TNB 2017 was different from that in 2016. The amplitudes in the 50–65 Hz band (blue line in **Figure 5A**) were high in February but then decreased until mid-April. However, the sound levels rebounded in May and reached high levels in July. The reason for the “noisy winter” in 2017 can be found in the wind speed and sea-ice concentration. In TNBP, the sea ice concentrations frequently dropped below 80% even in the austral winter seasons (**Figure 5C**), in contrast to that in the BI region (**Figure 4C**). This phenomenon is due to the blowing out of sea ice from the polynya by katabatic winds. Yoon et al. (2020) reported that the number

of katabatic wind events (the wind direction is westerly, and the wind speed exceeds 25 ms^{-1}) in TNBP was the highest in the 2017 austral winter (April–October) during the 2015–2017 period, and the polynya opened for the longest time period in 2017. **Figure 5C** shows that the sea ice concentration dropped most frequently in 2017. The frequent katabatic winds and high mobility of sea ice in open sea can make for a “noisy winter” in the polynya region in contrast to the silent winters in the BI region and other sea-ice regions, e.g., Beaufort Sea (Lewis and Denner, 1988; Kinda et al., 2013), Antarctic Peninsula (Dziak et al., 2010, 2015), and Atlantic sector of the Southern Ocean (Menze et al., 2017).

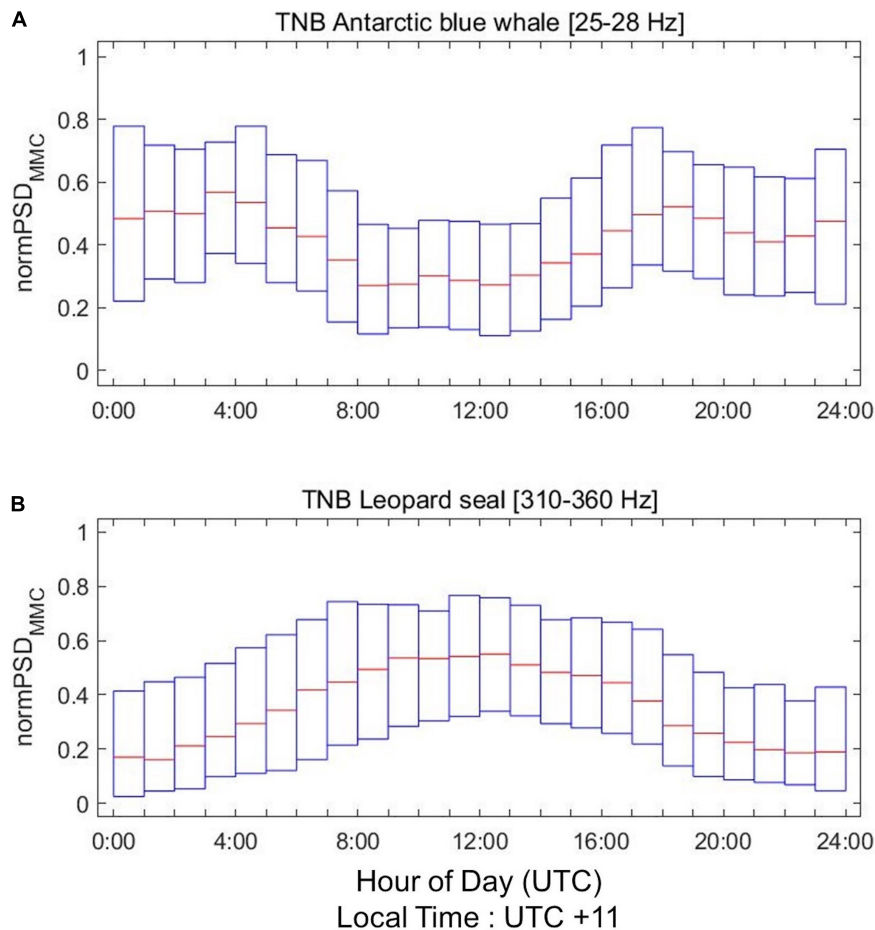


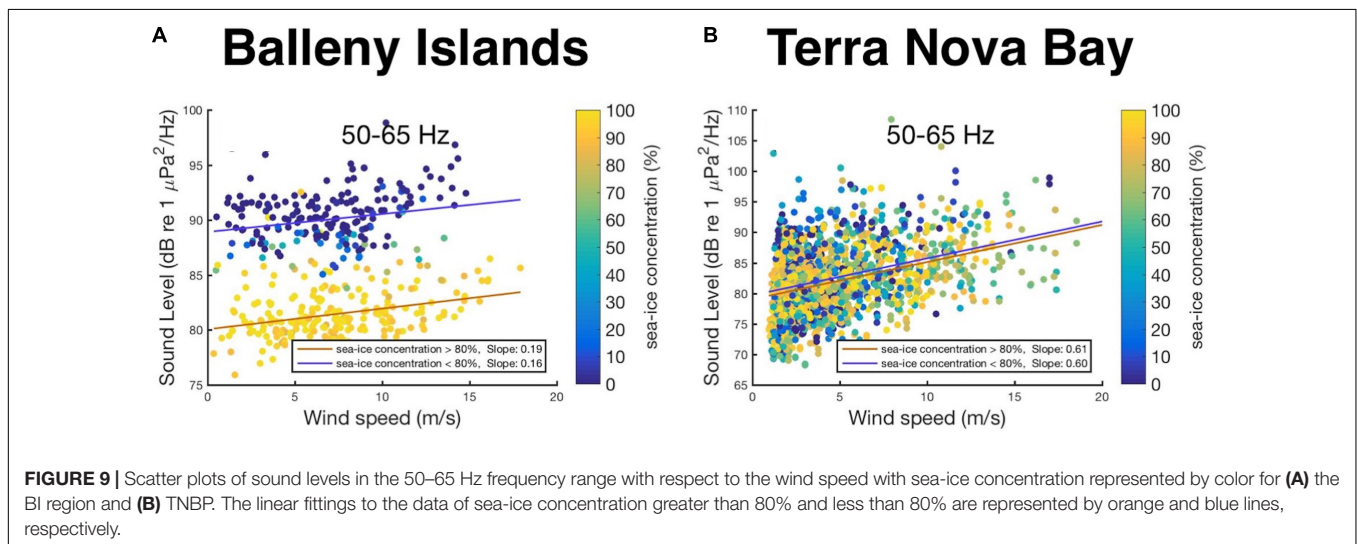
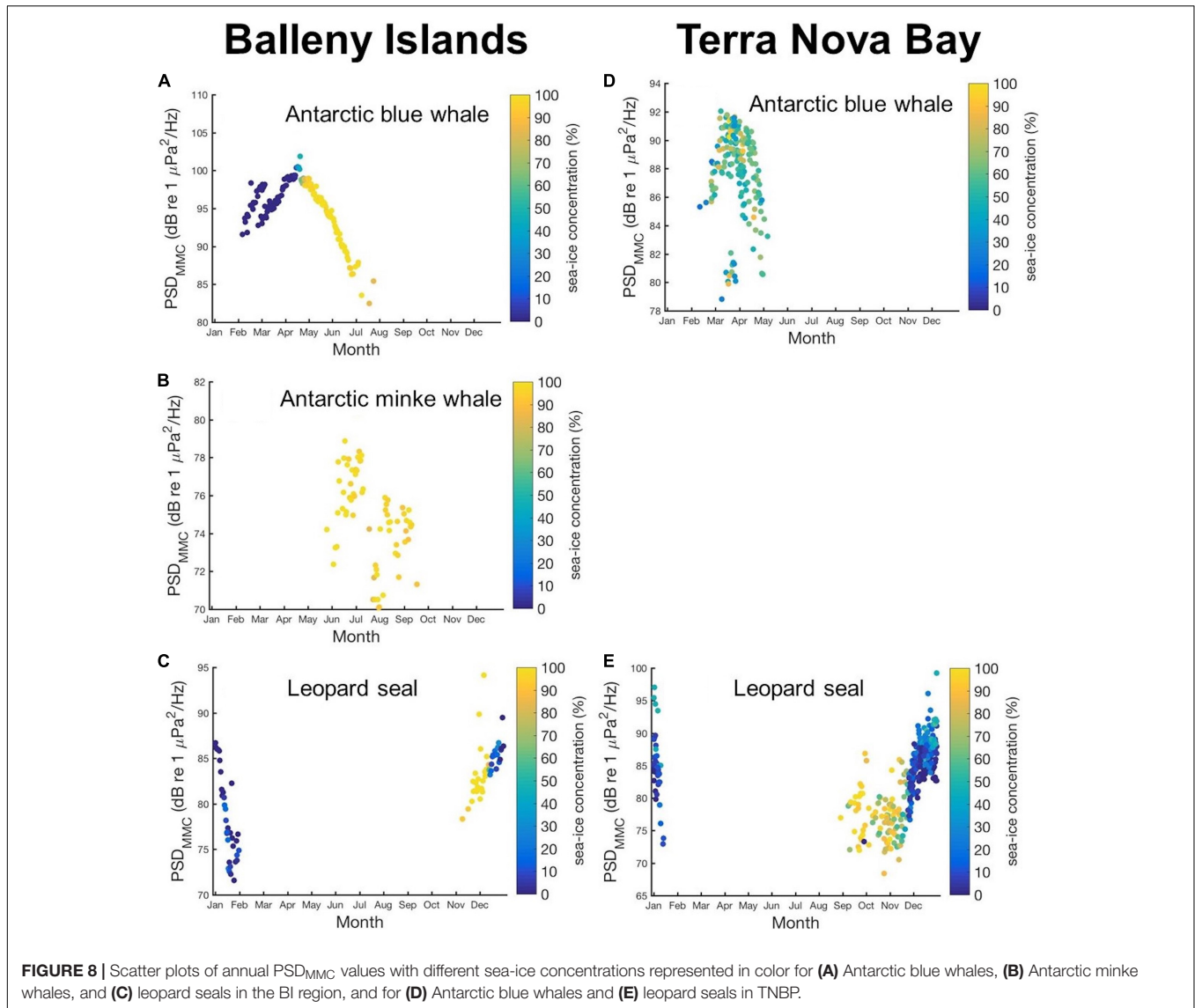
FIGURE 7 | Same as **Figure 6** but for the **(A)** Antarctic blue whales and **(B)** leopard seals in the TNBP.

In the TNBP, we estimate the PSD_{MMC} only for Antarctic blue whales and leopard seals (**Figure 5B**). Although we detected Antarctic minke whale signals in the TNBP (**Supplementary Figure 2D**), the PSD_{MMC} estimation could not proceed because upper fitting windows are influenced by vocalizations of leopard seals from late August (**Figure 5B**). The leopard seals' calls in the TNBP start earlier than those in the BI region and Atlantic sector of the Southern Ocean (Klinck, 2008; Van Opzeeland et al., 2010; Menze et al., 2017), and the chorus levels are remarkably loud. These results might be attributed to a higher density of leopard seals and year-round existence of pack ice in the polynya region, the inhabitation of leopard seals. Annual PSD_{MMC} values of Antarctic blue whales in TNB are conspicuous in March; however, the amplitude variations do not show any correlations with sea-ice concentrations and vary yearly (**Figure 5**).

We normalize the hourly PSD_{MMC} values between 0 and 1 for each day and plot them over a day to find diel patterns in the BI (**Figure 6**) and TNB (**Figure 7**) data. The PSD_{MMC} value of Antarctic blue whale is slightly lower at midnight than at midday in the BI region and TNBP (**Figures 6A, 7A**), corresponding to the diel pattern of the calling rate in Southern Indian Ocean (Leroy et al., 2016). The PSD_{MMC} value of Antarctic minke

whales in the BI region is increased at midnight (**Figure 6B**). Minke whales were observed to be more active in nighttime in Southern Ocean (Menze et al., 2017; Shabangu et al., 2020) and Northern Ocean (Risch et al., 2013, 2019), owing to the diurnal vertical migration of their prey (zooplankton) into deepwater during the day and to the surface at nighttime (Demer and Hewitt, 1995). However, the seasonal variation in the diel patterns was not significant in our study (**Supplementary Figure 5**). **Figures 6C, 7B** show the active calling of leopard seals during nighttime, which reduces in daytime. Similar diel patterns have been reported by previous studies (Thomas and DeMaster, 1982; Klinck, 2008; Van Opzeeland et al., 2010), and these patterns most likely arise from the haul-out behavior of the leopard seals that rest on ice during the solar midday.

To investigate the seasonal changes in the sea-ice concentration and their effects on the marine mammal vocalization, we plotted the daily averaged PSD_{MMC} values of Antarctic blue whales, Antarctic minke whales (only for the BI data), and leopard seals over the day of the year with sea ice concentration represented by color (**Figure 8**). The bimodal pattern of sea-ice concentrations in the BI region is clearly represented by a sudden color change from navy to yellow in



April, while the PSD_{MMC} value of Antarctic blue whales starts decreasing with a sudden change in sea-ice concentrations in the BI region (Figure 8A). Supplementary Figure 6 shows a scatterplot of the PSD_{MMC} values of Antarctic blue whales, together with the number of days that the sea ice concentration exceeded 80% in the last 100 days; the distance to the closest open sea has also been represented in different colors. Furthermore, whale sound levels diminish with an increase in the duration of the ice-covered period and the distance to the nearest open sea. This may be due to the migration of whales to find reliable access to open water for breathing (Van Opzeeland et al., 2013; Thomisch et al., 2016). The presence period of Antarctic blue whale calls in the TNBP is shorter than that in the BI region, and we found no persistent correlation of this result with the sea-ice concentrations in the TNBP (Figure 8E). The Antarctic minke whale calls are observed in the BI region from May to October when the sea ice concentration is higher than 70% (Figure 8B). The leopard seal PSD_{MMC} increasing from early November in the BI region and from late August in the TNBP, which resulted in an energy peak in late December that ceased to exist in February (Figures 8C,E).

The austral winter season (July–August) in the TNBP is another noisy period attributed to repeated storm noise and cryogenic signals as shown in the long-term spectrogram (Figures 2B,C, 5A). To determine the dominant environmental factor controlling low-frequency cryogenic noise, we created scatterplots of sound levels in the 50–65 Hz band over the wind speed with sea-ice concentration represented by color (Figure 9). The linear fittings to the data of sea-ice concentration greater than 80% and less than 80% are represented by orange and blue lines, respectively. Table 3 lists the slopes, intercepts of the fitting lines, and Pearson's correlation coefficients between the sound levels and the wind speed. In the BI region, the significant difference in the intercepts under the two sea-ice conditions (89 dB for $SIC < 80\%$; 80 dB for $SIC > 80\%$), gentle slopes, and low correlation coefficients indicate that the low-frequency cryogenic noise is dominantly controlled by sea-ice conditions in the BI region. In contrast, sea-ice concentration did not cause significant changes in TNB. The fitting lines for the two sea ice concentrations in TNB were largely the same, and the slopes and correlation coefficients were greater than those of the BI record. This implies that the vibration and fracturing of ice shelves related to strong winds could be a dominant source generating low-frequency noise in the TNBP rather than sea ice.

CONCLUSION

We reviewed soundscapes obtained from long-term hydroacoustic recording in two different regions of the Western Ross Sea, Antarctic: the BI region and TNBP.

The study showed that cryogenic events and marine mammals are the major sound sources in both regions. Tectonic earthquake and anthropogenic noises due to vessels were also found at various times in the spectrograms. The major marine mammal signals in the long-term spectrogram and SPDs of both regions are from Antarctic blue whales in the late summer–fall months

and leopard seals in early summer. Typical fin whale signals are not detected in both region despite there are peaks at 80 and 90 Hz in the SPD plots of the BI region. A fin whale chorus was observed between March and May in the BI recordings; however, it could not be identified in the TNB recordings, which is in accordance to the study conducted by Širović et al. (2009) in the Ross Sea. Antarctic minke whales calls are detected in both regions and peaked in austral winter season in the BI region reflecting their preference to dense sea-ice environments (Filun et al., 2020). We found humpback whale vocalization and long-duration (>200 s) downsweeps of unknown origin from 75 to 62 Hz in TNBP. Correlation with sea ice in the BI region reflects baleen whale behaviors such as high density in the ice margin and migrations to find reliable access to open water for breathing. The diel patterns associated with the vocalization of Antarctic blue whales (louder in daytime) and Antarctic minke whales (louder in nighttime) may be related to their feeding ecology. Louder vocalization of leopard seals in midnight results from their haul-out behavior.

The influences of wind and sea ice on ambient noise were different in the two regions. In the BI region, sea ice, often near 100% concentration, reduced ambient sound levels, similarly to other polar regions. However, the ambient noise in TNB increased due to strong winds, regardless of the sea-ice concentration; hence, the austral winter in 2017 was very noisy because of the frequent katabatic winds coming from the land. The regional differences seem to be attributed to the higher mobility of sea ice by the polynya process and the strong noise generated near ice shelves.

Although monitoring long-term soundscapes in extremely cold waters is challenging because of the logistical difficulties and harsh conditions at sea, it can significantly help understand the spatiotemporal changes in the Southern Ocean in the context of cryosphere changes, and can provide a means of assessing the status and trends of biodiversity in the Ross Sea region Marine Protected Area. Future intensive studies, which quantitatively measure the occurrence of individual species and cryogenic events as well as elucidate acoustic propagation by considering sea-ice and water temperature variations, will provide a better understanding of the soundscapes in Southern Ocean.

DATA AVAILABILITY STATEMENT

The raw hydroacoustic data used for this study can be downloaded through the Korea Polar Data Center (KPDC; <https://kpd.c.kopri.re.kr>) and the DOIs are as follows: <https://dx.doi.org/doi:10.22663/KOPRI-KPDC-00000830.4> (BAL15), <https://dx.doi.org/doi:10.22663/KOPRI-KPDC-00000750.3> (TNBS16), <https://dx.doi.org/doi:10.22663/KOPRI-KPDC-00000899.5> (TNBS17 and TNBN17), and <https://dx.doi.org/doi:10.22663/KOPRI-KPDC-00001171.4> (TNBS18 and TNBN18). The meteorological data in Jang Bogo Station during 2015–2018 are available upon request at the KPDC site, and the DOIs are as follows: <https://dx.doi.org/doi:10.22663/KOPRI-KPDC-00000543.1> (2015), <https://dx.doi.org/doi:10.22663/KOPRI-KPDC-00000643.1> (2016),

<https://dx.doi.org/doi:10.22663/KOPRI-KPDC-00001150.1> (2017), and <https://dx.doi.org/doi:10.22663/KOPRI-KPDC-00001151.1> (2018). ERA5 data are available through the ECMWF website (<http://www.ecmwf.int/>), sea-ice concentration data through the University of Bremen (<http://www.iup.uni-bremen.de/seaice/amsr/>), and sea-ice extent data through the National Snow and Ice Data Center (<https://nsidc.org/data/G02135>). Data analysis codes are available through the Zenodo digital repository (<https://doi.org/10.5281/zenodo.5567347>).

AUTHOR CONTRIBUTIONS

WSL, RPD, JKH, and YP were principal investigators on Ross sea hydrophone projects. SY designed this study and prepared the figure and manuscript. RPD, HM, T-KL, and JHH designed the hydroacoustic experiments. SY, LR, WSL, JHH, and S-GK led at-sea hydrophone deployments. LR and T-KL performed data quality control. T-KL, JHH, SY, and WSL developed data processing programs. SY, WSL, RPD, HM, JHH, S-GK, and AS processed and analyzed the data. DKM, AS, HM, and SY identified bio-acoustic signals. All authors contributed to manuscript edits.

FUNDING

This work was sponsored by a research grant from the Korean Ministry of Oceans and Fisheries (KIMST20190361; PM21020), the Korea Polar Research Institute (PE21050), and the NOAA/Pacific Marine Environmental Laboratory contribution number 5254.

ACKNOWLEDGMENTS

We thank the captain and crew of R/V *Araon*, J. Lee, M. Fowler, and S. Nieuwkirk for the deployment and recovery of hydrophone arrays. We also thank T. Choi, ECMWF, University of Bremen, NSIDC for sharing their meteorological and sea ice data. We also thank the reviewers CW and SM as well as the topical editor for the review, which greatly improved this manuscript.

SUPPLEMENTARY MATERIAL

The Supplementary Material for this article can be found online at: <https://www.frontiersin.org/articles/10.3389/fmars.2021.703411/full#supplementary-material>

REFERENCES

- Andrew, R. K., Howe, B. M., and Mercer, J. A. (2011). Long-time trends in ship traffic noise for four sites off the North American West Coast. *J. Acoust. Soc. Am.* 129, 642–651. doi: 10.1121/1.3518770
- Andrew, R. K., Howe, B. M., Mercer, J. A., and Dzieciuch, M. A. (2002). Ocean ambient sound: comparing the 1960s with the 1990s for a receiver off the California coast. *Acoust. Res. Lett. Online* 3, 65–70. doi: 10.1121/1.1461915

Supplementary Figure 1 | (left) Sound speed profiles in the TNB region in December (A) and March (B), and (right) the transmission loss calculated by KRAKEN (Porter, 1992) at 25 and 400 Hz. The sound speed profiles are calculated from the conductivity, temperature, and depth (CTD) measurements performed by the icebreaker R/V *Araon* (Dziak et al., 2019). Blue solid lines represent the transmission loss in a 400 m deep receiver when the sound source is at a depth of 50 m in the case of a flat sea surface with a flat bottom.

Supplementary Figure 2 | Spectrograms of the various acoustic sources recorded in the BI region or TNBP as shown above each spectrogram: (A) earthquake (T-phase) and impulsive icequakes; (B) baleen whale calls and noise in the BI region; (C) biotid sounds from Antarctic minke whale in the BI region; (D) leopard seal sound in the 200–400 Hz band, biotid sounds of Antarctic minke whale in the 120–250 Hz, and Antarctic blue whale's "D-calls" in 50–100 Hz; (E) a "chorus" of Antarctic blue whales (Thomisch et al., 2016) at around 27 Hz and 18 Hz; (F) broadband storm noise continued for several hours and anthropogenic noise from a ship that continued for several days; (G) leopard seals and humpback whale vocalizations; (H) undefined downsweeps continued hundreds of seconds.

Supplementary Figure 3 | Examples of ambient sound spectrum with marine mammal contributions (MMC) from Antarctic blue whales, Antarctic minke whales, and leopard seals for the BI (BAL15) and TNB (TNBN17) regions. Measured power spectral density (PSD) (black line) and fitted interpolation functions in the frequency bands associated with Antarctic blue whales (red), Antarctic minke whales (olive green), and leopard seals (green). PSD_{MMC} values are estimated in the shaded frequency bands by using the method adopted by Menze et al. (2017). (A) Averaged PSD_{MMC} recorded in BAL15 on 2015.06.20 from 12:00 to 13:00 and the fitted interpolation functions for bands associated with Antarctic blue whales and minke whales. Note that the PSD_{MMC} values of Antarctic minke whales is estimated only for the BAL15 data from February to September, where the upper fitting band (300–351 Hz) is stable due to the absence of sounds emitted by leopard seals. (B) Averaged PSD_{MMC} recorded in BAL15 on 2015.12.10 from 12:00 to 13:00 and the fitted interpolation functions for the band associated with leopard seals. PSD_{MMC} values of leopard seals in the BI region are estimated from October to January, where the lower fitting band (39–161 Hz) is stable in the absence of Antarctic minke whale calls. (C) Averaged PSD_{MMC} recorded in TNBN17 on 2017.03.15 from 12:00 to 13:00 and fitted interpolation functions for Antarctic blue whales. Owing to the big fluctuation under 18 Hz and the superposed sound energy from various sources in the neighboring frequency band, a narrower fitting band than that applied to the BI data is adopted. (D) Averaged PSD_{MMC} recorded in TNBN17 on 2017.12.10 from 20:00 to 21:00 (solid black line) and on 2017.08.20 from 12:00 to 13:00 (dashed black line), and the fitted interpolation functions for leopard seals. We could not calculate the MMC of Antarctic minke whales in the TNBP, as leopard seals produced sounds from late August.

Supplementary Figure 4 | Zoomed-in spectrogram of **Supplementary Figure 2B**, with a frequency range of 1–40 Hz and different color scales. Number of signals exist at two frequency bands: 17–22 and 25–29 Hz.

Supplementary Figure 5 | Seasonal variation of the diel patterns in the PSD_{MMC} values of Antarctic minke whales in the BI region.

Supplementary Figure 6 | Scatterplot of PSD_{MMC} values of Antarctic blue whales in the BI region, together with the number of days that the sea-ice concentration exceeded 80% in the last 100 days. Distances to the closest open sea are represented in different colors.

- Brierley, A. S., Fernandes, P. G., Brandon, M. A., Armstrong, F., Millard, N. W., Mcphail, S. D., et al. (2002). Antarctic krill under sea ice: elevated abundance in a narrow band just south of ice edge. *Science* 295, 1890–1892. doi: 10.1126/science.1068574
- Castellote, M., Clark, C. W., and Lammers, M. O. (2012). Acoustic and behavioural changes by fin whales (*Balaenoptera physalus*) in response to shipping and airgun noise. *Biol. Conserv.* 147, 115–122. doi: 10.1016/j.biocon.2011.2.021

- Chapman, N. R., and Price, A. (2011). Low frequency deep ocean ambient noise trend in the northeast Pacific Ocean. *J. Acoust. Soc. Am.* 129, EL161–EL165. doi: 10.1121/1.3567084
- Chaput, J., Aster, R. C., Mcgrath, D., Baker, M., Anthony, R. E., Gerstoft, P., et al. (2018). Near-surface environmentally forced changes in the Ross Ice Shelf observed with ambient seismic noise. *Geophys. Res. Lett.* 45:196. doi: 10.1029/2018GL079665
- Clark, C. W., Ellison, W. T., Southall, B. L., Hatch, L., Van Parijs, S. M., Frankel, A., et al. (2009). Acoustic masking in marine ecosystems: intuitions, analysis, and implication. *Mar. Ecol. Prog. Ser.* 395, 201–222. doi: 10.3354/meps08402
- de la Mare, W. K. (1997). Abrupt mid-twentieth-century decline in Antarctic sea-ice extent from whaling records. *Nature* 389, 57–60. doi: 10.1038/37956
- Demer, D. A., and Hewitt, R. P. (1995). Bias in acoustic biomass estimates of *Euphausia superba* due to diel vertical migration. *Deep Sea Res. Oceanogr. Res. Paper* 42, 455–475. doi: 10.1016/0967-0637(94)E0005-C
- Dziak, R. P., Bohnenstiehl, D. R., Stafford, K. M., Matsumoto, H., Park, M., Lee, W. S., et al. (2015). Sources and levels of ambient ocean sound near the Antarctic Peninsula. *PLoS One* 10:e0123425. doi: 10.1371/journal.pone.0123425
- Dziak, R. P., Hong, J., Kang, S.-G., Lau, T.-K., Haxel, J. H., and Matsumoto, H. (2017). “The Balleny island hydrophone array: hydro-acoustic records of sea-ice dynamics, seafloor volcano-tectonic activity, and marine mammal vocalizations off Antarctica,” in *Proceedings of the OCEANS 2017-Aberdeen*, (Aberdeen: IEEE), 1–8. doi: 10.1109/OCEANSE.2017.8084571
- Dziak, R. P., Lee, W. S., Haxel, J. H., Matsumoto, H., Tepp, G., Lau, T.-K., et al. (2019). Hydroacoustic, meteorologic and seismic observations of the 2016 Nansen ice shelf calving event and iceberg formation. *Front. Earth Sci.* 7:183. doi: 10.3389/feart.2019.00183
- Dziak, R. P., Park, M., Lee, W. S., Matsumoto, H., Bohnenstiehl, D. R., and Haxel, J. H. (2010). Tectonomagmatic activity and ice dynamics in the Bransfield Strait back-arc basin, Antarctica. *J. Geophys. Res.* 115:B01102. doi: 10.1029/2009JB006295
- Edds-Walton, P. L. (1997). Acoustic communication signals of mysticete whales. *Bioacoustics* 8, 47–60. doi: 10.1080/09524622.1997.9753353
- Erbe, C., Dunlop, R., Jenner, K. C. S., Jenner, M.-N., Mccauley, R. D., Parnum, I., et al. (2017). Review of underwater and in-air sounds emitted by Australian and Antarctic marine mammals. *Acoust. Aust.* 45, 179–241. doi: 10.1007/s40857-017-0101-z
- Fetterer, F., Knowles, K., Meier, W. N., and Savoie, M. (2002). *Sea Ice Index, Version 1*. Boulder, CO: National Snow and Ice Data Center, doi: 10.7265/N5QJ7F7W
- Filun, D., Thomisch, K., Boebel, O., Brey, T., Širović, A., Spiessicke, S., et al. (2020). Frozen verses: Antarctic minke whales (*Balaenoptera bonaerensis*) call predominantly during austral winter. *R. Soc. Open Sci.* 7:192112. doi: 10.1098/rsos.192112
- Fox, C. G., Matsumoto, H., and Lau, T.-K. A. (2001). Monitoring Pacific Ocean seismicity from an autonomous hydrophone array. *J. Geophys. Res.* 106, 4183–4206. doi: 10.1029/2000JB900404
- Frisk, G. V. (2012). Noiseconomics: the relationship between ambient noise levels in the sea and global economic trends. *Sci. Rep.* 2:437. doi: 10.1038/srep00437
- Fusco, G., Flocco, D., Budillon, G., Spezie, G., and Zambianchi, E. (2002). Dynamics and variability of Terra nova Bay polynya. *Mar. Ecol.* 23, 201–209. doi: 10.1111/j.1439-0485.2002.tb00019.x
- Glowacki, O., and Deane, G. B. (2020). Quantifying iceberg calving fluxes with underwater noise. *Cryosphere* 14, 1025–1042. doi: 10.5194/tc-14-1025-2020
- Glowacki, O., Deane, G. B., Moskalik, M., Blondel, P., Tegowski, J., and Blaszczyk, M. (2015). Underwater acoustic signatures of glacier calving. *Geophys. Res. Lett.* 42, 804–812. doi: 10.1002/2014GL062859
- Haver, S. M., Klinck, H., Nieuwkerk, S. L., Matsumoto, H., Dziak, R. P., and Miksis-Olds, J. L. (2017). The not-so-silent world: measuring Arctic, equatorial, and Antarctic soundscapes in the Atlantic Ocean. *Deep Sea Res. Oceanogr. Res. Paper* 122, 95–104. doi: 10.1016/j.dsr.2017.03.002
- Hersbach, H., Bell, B., Berrisford, P., Hirahara, S., Horányi, A., Muñoz-Sabater, J., et al. (2020). The ERA5 global reanalysis. *Q. J. Roy. Meteorol. Soc.* 146, 1999–2049. doi: 10.1002/qj.3803
- Kinda, G. B., Simard, Y., Gervaise, C., Mars, J. I., and Fortier, L. (2013). Under-ice ambient noise in eastern Beaufort Sea, Canadian Arctic, and its relation to environmental forcing. *J. Acoust. Soc. Am.* 134, 77–87. doi: 10.1121/1.480833
- Klinck, H. (2008). *Automated Passive Acoustic Detection, Localization and Identification of Leopard Seals: From Hydro-Acoustic Technology to Leopard Seal Ecology*. Bremerhaven: Alfred Wegener Institute for Polar and Marine Research.
- Knudsen, V. O., Alford, R., and Emling, J. (1948). Underwater ambient noise. *J. Mar. Res.* 7, 410–429.
- Kurtz, D. D., and Bromwich, D. H. (1985). “A recurring, atmospherically forced Polynya in Terra Nova Bay,” in *Oceanology of the Antarctic Continental Shelf*, ed. S. S. Jacobs (Washington, DC: American Geophysical Union), 177–201. doi: 10.1029/AR043p0177
- Leroy, E. C., Samaran, F., Bonnel, J., and Royer, J. Y. (2016). Seasonal and diel vocalization patterns of Antarctic blue whale (*Balaenoptera musculus intermedia*) in the Southern Indian ocean: a multi-year and multi-site study. *PLoS One* 11:e0163587. doi: 10.1371/journal.pone.0163587
- Lewis, J. K., and Denner, W. W. (1988). Arctic ambient noise in the Beaufort Sea: seasonal relationships to sea ice kinematics. *J. Acoust. Soc. Am.* 83, 549–565. doi: 10.1121/1.396149
- Ljungblad, D. K., Clark, C. W., and Shimada, H. (1998). A comparison of sounds attributed to pygmy blue whales (*Balaenoptera musculus breviceauda*) recorded south of the Madagascar Plateau and those attributed to true blue whales (*Balaenoptera musculus*) recorded off Antarctica. *Rep. Int. Whal. Comm.* 48, 439–442.
- MacAyeal, D. R., Okal, E. A., Aster, R. C., and Bassis, J. N. (2008). Seismic and hydroacoustic tremor generated by colliding icebergs. *J. Geophys. Res.* 113:F03011. doi: 10.1029/2008JF001005
- Matsinos, Y. G., Tsaligopoulos, A., and Economou, C. (2016). The interdisciplinary development of the Term “soundscape”; tracing its ecological roots. *AEgean J. Environ. Sci.* 2, 11–23.
- Matsumoto, H., Bohnenstiehl, D. R., Tournadre, J., Dziak, R. P., Haxel, J. H., Lau, T.-K. A., et al. (2014). Antarctic icebergs: a significant natural ocean sound source in the southern hemisphere. *Geochem. Geophys. Geosyst.* 15, 3448–3458. doi: 10.1002/2014GC005454
- McDonald, M. A., Hildebrand, J. A., and Wiggins, S. M. (2006). Increases in deep ocean ambient noise in the northeast Pacific west of San Nicolas Island, California. *J. Acoust. Soc. Am.* 120, 711–718. doi: 10.1121/1.2216565
- Menze, S., Zitterbart, D. P., Van Opzeeland, I., and Boebel, O. (2017). The influence of sea ice, wind speed and marine mammals on Southern Ocean ambient sound. *R. Soc. Open Sci.* 4:160370. doi: 10.1098/rsos.160370
- Miksis-Olds, J. L., Bradley, D. L., and Niu, X. M. (2013). Decadal trends in Indian Ocean ambient sound. *J. Acoust. Soc. Am.* 134, 3464–3475. doi: 10.1121/1.4821537
- Miller, B. S., Balcazar, N., Nieuwkerk, S., Leroy, E. C., Aulich, M., Shabangu, F. W., et al. (2021). An open access dataset for developing automated detectors of Antarctic baleen whale sounds and performance evaluation of two commonly used detectors. *Sci. Rep.* 11:806. doi: 10.1038/s41598-020-78995-8
- Moore, S. E., Stafford, K. M., Melling, H., Berchok, C., Wiig, Ø, Kovacs, K. M., et al. (2012). Comparing marine mammal acoustic habitats in Atlantic and Pacific sectors of the high Arctic: year-long records from Fram Strait and the Chukchi Plateau. *Polar Biol.* 35, 475–480. doi: 10.1007/s00300-011-1086-y
- Morlighem, M., Rignot, E., Binder, T., Blankenship, D., Drews, R., Eagles, G., et al. (2020). Deep glacial troughs and stabilizing ridges unveiled beneath the margins of the Antarctic ice sheet. *Nat. Geosci.* 13, 132–137. doi: 10.1038/s41561-019-0510-8
- Payne, R. S., and McVay, S. (1971). Songs of humpback whales. *Science* 173, 585–597. doi: 10.1126/science.173.3997.585
- Pettit, E. C. (2012). Passive underwater acoustic evolution of a calving event. *Ann. Glaciol.* 53, 113–122. doi: 10.3189/2012AoG60A137
- Pettit, E. C., Nystuen, J. A., and O’Neil, S. (2012). Listening to glaciers: passive hydroacoustics near marine-terminating glaciers. *Oceanography* 25, 104–105. doi: 10.5670/oceanog.2012.81
- Porter, M. B. (1992). *The KRACKEN Normal Mode Program*. Washington, DC: Naval Research Lab.
- Risch, D., Clark, C. W., Dugan, P. J., Popescu, M., Siebert, U., and Van Parijs, S. M. (2013). Minke whale acoustic behavior and multi-year seasonal and diel vocalization patterns in Massachusetts Bay, USA. *Mar. Ecol. Prog. Ser.* 489, 279–295. doi: 10.3354/meps10426
- Risch, D., Gales, N. J., Gedamke, J., Kindermann, L., Nowacek, D. P., Read, A. J., et al. (2014). Mysterious bio-duck sound attributed to the Antarctic minke

- whale (*Balaenoptera bonaerensis*). *Biol. Lett.* 10:20140175. doi: 10.1098/rsbl.2014.0175
- Risch, D., Wilson, S. C., Hoogerwerf, M., Van Geel, N. C. F., Edwards, E. W. J., and Brookes, K. L. (2019). Seasonal and diel acoustic presence of North Atlantic minke whales in the North Sea. *Sci. Rep.* 9:3571. doi: 10.1038/s41598-019-39752-8
- Rogers, T. L., Cato, D. H., and Bryden, M. M. (1996). Behavioral significance of underwater vocalizations of captive leopard seals, *Hydrurga leptonyx*. *Mar. Mamm. Sci.* 12, 414–427. doi: 10.1111/j.1748-7692.1996.tb00593.x
- Sansiviero, M., Morales Maqueda, M. Á, Fusco, G., Aulicino, G., Flocco, D., and Budillon, G. (2017). Modelling sea ice formation in the Terra nova Bay polynya. *J. Mar. Syst.* 166, 4–25. doi: 10.1016/j.jmarsys.2016.06.013
- Schafer, R. M. (1969). *The New Soundscape: A Handbook for the Modern Music Teacher*. Boisbriand, QC: BMI Canada Limited Don Mills.
- Shabangu, F. W., Findlay, K., and Stafford, K. M. (2020). Seasonal acoustic occurrence, diel-vocalizing patterns and biouck call-type composition of Antarctic minke whales off the west coast of South Africa and the Maud Rise, Antarctica. *Mar. Mam. Sci.* 36, 658–675. doi: 10.1111/mms.12669
- Širović, A., Hildebrand, J. A., and Wiggins, S. M. (2007). Blue and fin whale call source levels and propagation range in the Southern Ocean. *J. Acoust. Soc. Am.* 122, 1208–1215. doi: 10.1121/1.2749452
- Širović, A., Hildebrand, J. A., Wiggins, S. M., McDonald, M. A., Moore, S. E., and Thiele, D. (2004). Seasonality of blue and fin whale calls and the influence of sea ice in the western Antarctic Peninsula. *Deep Sea Res. 2 Top. Stud. Oceanogr.* 51, 2327–2344. doi: 10.1016/j.dsr2.2004.08.005
- Širović, A., Hildebrand, J. A., Wiggins, S. M., and Thiele, D. (2009). Blue and fin whale acoustic presence around Antarctica during 2003 and 2004. *Mar. Mamm. Sci.* 25, 125–136. doi: 10.1111/j.1748-7692.2008.00239.x
- Southwell, C., Kerry, K., Ensor, P., Woehler, E. J., and Rogers, T. (2003). The timing of pupping by pack-ice seals in East Antarctica. *Polar Biol.* 26, 648–652. doi: 10.1007/s00300-003-0534-8
- Spreen, G., Kaleschke, L., and Heygster, G. (2008). Sea ice remote sensing using AMSR-E 89-GHz channels. *J. Geophys. Res.* 113:C02S03. doi: 10.1029/2005JC00b3384
- Stevens, C., Lee, W. S., Fusco, G., Yun, S., Grant, B., Robinson, N., et al. (2017). The influence of the Drygalski Ice Tongue on the local ocean. *Ann. Glaciol.* 58, 51–59. doi: 10.1017/aog.2017.4
- Thomas, J. A., and DeMaster, D. P. (1982). An acoustic technique for determining diurnal activities in leopard (*Hydrurga leptonyx*) and crabeater (*Lobodon carcinophagus*) seal. *Can. J. Zool.* 60, 2028–2031. doi: 10.1139/z82-260
- Thomisch, K., Boebel, O., Clark, C. W., Hagen, W., Spiesecke, S., Zitterbart, D. P., et al. (2016). Spatio-temporal patterns in acoustic presence and distribution of Antarctic blue whales *Balaenoptera musculus intermedia* in the Weddell Sea. *Endanger. Species Res.* 30, 239–253. doi: 10.3354/esr00739
- Van Opzeeland, I., Van Parijs, S., Kindermann, L., Burkhardt, E., and Boebel, O. (2013). Calling in the cold: pervasive acoustic presence and distribution of humpback whales (*Megaptera novaeangliae*) in Antarctic coastal waters. *PLoS One* 8:e73007. doi: 10.1371/journal.pone.0073007
- Van Opzeeland, I., Van Parijs, S. M., Bornemann, H., Frickenhaus, S., Kindermann, L., Klinck, H., et al. (2010). Acoustic ecology of Antarctic pinnipeds. *Mar. Ecol. Prog. Ser.* 414, 267–291. doi: 10.3354/meps08683
- Watkins, W. A., Tyack, P., Moore, K. E., and Bird, J. E. (1987). The 20-Hz signals of finback whales (*Balaenoptera physalus*). *J. Acoust. Soc. Am.* 82, 1901–1912. doi: 10.1121/1.395685
- Wenz, G. M. (1962). Acoustic ambient noise in the ocean: spectra and sources. *J. Acoust. Soc. Am.* 34, 1936–1956. doi: 10.1121/1.1909155
- Yoon, S.-T., Lee, W. S., Stevens, C., Jendersie, S., Nam, S., Yun, S., et al. (2020). Variability in high-salinity shelf water production in the Terra nova Bay polynya, Antarctica. *Ocean Sci.* 16, 373–388. doi: 10.5194/os-16-373-2020

Conflict of Interest: The authors declare that the research was conducted in the absence of any commercial or financial relationships that could be construed as a potential conflict of interest.

Publisher's Note: All claims expressed in this article are solely those of the authors and do not necessarily represent those of their affiliated organizations, or those of the publisher, the editors and the reviewers. Any product that may be evaluated in this article, or claim that may be made by its manufacturer, is not guaranteed or endorsed by the publisher.

Copyright © 2021 Yun, Lee, Dziak, Roche, Matsumoto, Lau, Sremba, Mellinger, Haxel, Kang, Hong and Park. This is an open-access article distributed under the terms of the Creative Commons Attribution License (CC BY). The use, distribution or reproduction in other forums is permitted, provided the original author(s) and the copyright owner(s) are credited and that the original publication in this journal is cited, in accordance with accepted academic practice. No use, distribution or reproduction is permitted which does not comply with these terms.